Journal of Anatomy

J. Anat. (2015) **226**, pp530–541 doi: 10.1111/joa.12306

Medial gastrocnemius muscle growth during adolescence is mediated by increased fascicle diameter rather than by longitudinal fascicle growth

Guido Weide,[1,2] Peter A. Huijing,[1] Josina C. Maas,[2] Jules G. Becher,[2] Jaap Harlaar[2] and Richard T. Jaspers[1]

[1]*Faculty of Human Movement Sciences, Laboratory for Myology, MOVE Research Institute Amsterdam, VU University Amsterdam, Amsterdam, The Netherlands*

[2]*Department of Rehabilitation Medicine, MOVE Research Institute Amsterdam, VU University Medical Center, Amsterdam, The Netherlands*

Abstract

Using a cross-sectional design, the purpose of this study was to determine how pennate gastrocnemius medialis (GM) muscle geometry changes as a function of adolescent age. Sixteen healthy adolescent males (aged 10–19 years) participated in this study. GM muscle geometry was measured within the mid-longitudinal plane obtained from a 3D voxel-array composed of transverse ultrasound images. Images were taken at footplate angles corresponding to standardised externally applied footplate moments (between 4 Nm plantar flexion and 6 Nm dorsal flexion). Muscle activity was recorded using surface electromyography (EMG), expressed as a percentage of maximal voluntary contraction (%MVC). To minimise the effects of muscle excitation, EMG inclusion criteria were set at $< 10\%$ of MVC. In practice, however, normalised EMG levels were much lower. For adolescent subjects with increasing ages, GM muscle (belly) length increased due to an increase in the length component of the physiological cross-sectional area measured within the mid-longitudinal plane. No difference was found between fascicles at different ages, but the aponeurosis length and pennation angle increased by 0.5 cm year^{-1} and 0.5 ° per year, respectively. Footplate angles corresponding to externally applied 0 and 4 Nm plantarflexion moments were not associated with different adolescent ages. In contrast, footplate angles corresponding to externally applied 4 and 6 Nm dorsal flexion moments decreased by 10 ° between 10 and 19 years. In conclusion, we found that in adolescents' pennate GM muscles, longitudinal muscle growth is mediated predominantly by increased muscle fascicle diameter.

Key words: adolescents; development; gastrocnemius medialis; growth; hypertrophy; muscle geometry; physiological cross-sectional area; ultrasound imaging.

Introduction

Skeletal muscles have the ability to adapt size and length–force characteristics to meet functional demands in daily life. During the process of maturation, skeletal muscles need to adapt in length to accommodate for bone growth (Haines, 1932), and they increase in their physiological cross-sectional area (PCSA) to generate sufficient force over a muscular length range corresponding to the required range of joint motion in daily life movements.

Correspondence
Richard T. Jaspers, Faculty of Human Movement Sciences, Laboratory for Myology, MOVE Research Institute Amsterdam, VU University Amsterdam, Van der Boechorststraat 9, 1081 BT Amsterdam, The Netherlands.
T: 00 31 20 5988463; E: r.t.jaspers@vu.nl

Accepted for publication *3 March 2015*
Article published online *16 April 2015*

Length–force characteristics of a muscle can typically be described by optimum length, active slack length and length range of active force exertion, as well as optimal active force. However, *in vivo*, the feasibility of assessing such variables is extremely low. Major morphological determinants of variables of muscle length–force characteristics are muscle physiological cross-sectional area, muscle fibre length (i.e. number of sarcomeres arranged in series) and lengths of serial elastic components (aponeurosis and tendon), as well as the angle of pennation [γ(fasc); Huijing, 1985]. Morphological assessment of muscle geometry *in vivo* is feasible using ultrasound imaging (Kawakami et al. 1993; Bénard et al. 2009).

Recent application of ultrasound imaging has enhanced insight regarding childhood growth of human m. gastrocnemius medialis (GM). During childhood (5–12 years), GM develops by uniform scaling: both fascicle length [ℓ(fasc)] and length component of physiological cross-sectional

area (ℓAf) increase, without any change in γ(fasc) (Bénard et al. 2011). In adolescents, growth mechanisms may be different from that of childhood, as from the onset of puberty, sex hormones play an important role in tissue and organ growth (Round, 1999). During human adolescence, the muscle belly length, and tendon and fascicle length of knee-extensors (mm. vastii medialis/intermedius/lateralis as well as of m. rectus femoris) and m. gastrocnemius lateralis (GL) are reported to increase proportionally (Morse et al. 2008; O'Brien et al. 2010). However, relative increases in Af are bigger than those of fascicle length (Morse et al. 2008; O'Brien et al. 2010). Previous to ultrasound imaging techniques becoming widely available, most knowledge regarding changes in muscle geometry during adolescent growth has been derived from animal studies. During pre-adolescent development, for rats, an increase of GM muscle belly length is achieved without addition of sarcomeres in series [i.e. increase in ℓ(fasc); Woittiez et al. 1986; De Koning et al. 1987; Heslinga & Huijing, 1990]. During adolescence, serum levels of growth factors are increased (Clark & Rogol, 1996; Rogol et al. 2002). For *ex vivo* cultured mature muscle fibres, such growth factors induce hypertrophy, and no addition of sarcomeres in series (Jaspers et al. 2008; Watt et al. 2010). Therefore, if elevated serum levels of growth factors are involved in muscle development, their effects are likely to appear as hypertrophy rather than as addition of sarcomeres in series.

The main objective of the present study was to investigate how human GM muscle geometry adapts during adolescence, and to investigate whether these adaptations involve muscle fascicle length increases, as seen in children, or exclusively involve muscle trophy effects increasing physiological cross-sectional area (Af), as seen in adolescent rats. We hypothesised that GM longitudinal growth is mediated by an increase in the length component of the physiological cross-sectional area of the muscle rather than by an increase in fascicle length.

Materials and methods

Subjects

Sixteen male Caucasian participants aged between 10 and 19 years volunteered to participate in this study. Before participating, subjects and parents (if subjects aged younger than 18 years) were informed about the nature of the experiment and signed for informed consent. The study complies with the declaration of Helsinki, and was approved by the Faculty of Human Movement Sciences Ethics Committee. Prior to participation in this study, it was established that participants were free of major physical disorders and were not involved in training that might have dramatically affected muscular hypertrophy. Growth effects during adolescence were studied on participants with ages ranging from 10 to 19 years, as full epiphyseal unions of lower limb long bones are confirmed at the age of 20 years (Cardoso, 2008).

Anthropometry

For all subjects, measurements were performed by the same assessor. Prior to subsequent assessments, body height and body mass were measured, and tibia length ℓ(tib) of the target leg was approximated as the mean of distances measured medially and laterally from the tibia plateau to the most prominent spot of the malleolus on the appropriate side.

Gonio-dynamometer: externally applied ankle moments induced footplate angles

Footplate angles attained in response to different external moments applied on the footplate were quantified to assess characteristics of the GM muscle. Subjects were lying prone on a examination table with both feet protruding over the edge (i.e. free movements at the ankle). The right leg was positioned centrally on the table with the tibia aligned horizontally. If needed, supports were used to elevate the distal part of the lower leg to attain such alignment (Fig. 1a). Measurements were performed using a custom-designed apparatus (Bénard et al. 2010), consisting of an adjustable footplate and a torque wrench equipped with an inclinometer (below referred to as the gonio-dynamometer; Huijing et al. 2013). The gonio-dynamometer could be docked in the footplate (Fig. 1a) and move the ankle (i.e. angle-fixator detached). Dorsal flexion angle and moments are indicated as positive values.

The adjustable footplate allows adjustments aimed at fixing the subtalar joint during footplate rotations (for details, see Huijing et al. 2013). Externally moments or footplate angles were either applied or measured for a total of five conditions in the following order: (i) footplate angle corresponding to 0 Nm ($\varphi_{0\ Nm}$); (ii) footplate angle corresponding to −4 Nm ($\varphi_{plantar\ -4\ Nm}$); (iii) footplate angle corresponding to 4 Nm ($\varphi_{dorsal\ 4\ Nm}$); (iv) externally applied moment corresponding to 0 ° footplate angle; (v) footplate angle corresponding to 6 Nm ($\varphi_{dorsal\ 6\ Nm}$). For each condition, measurements were repeated eight times, each held for 5 seconds, with 5 seconds rest in between. In order to minimise the effects of hysteresis, 2 minutes of rest was taken between consecutive measurement conditions.

Three-dimensional ultrasound imaging

Based on moment–angle footplate results, ultrasound scans of a part of GM volume were collected at 0 Nm ($\varphi_{0\ Nm}$) and 6 Nm ($\varphi_{dorsal\ 6\ Nm}$) dorsal flexion moment exerted. From these ultrasound scans, mid-longitudinal images were reconstructed to examine muscle geometry. Three-dimensional ultrasound imaging was preferred over a more conventional 2D approach because of pilot work indicating improved results for the 3D approach. Table 1 shows the results for two human cadavers, comparing 2D and 3D ultrasound techniques to anatomical measurements after dissection.

Footplate angles were fixed at the angle corresponding to the footplate angle–moment measurements (Fig. 1a). Once fixed, a continuous ultrasound scan was made along the middle of the muscle belly towards the distal end of the tendon with the ultrasound transducer in a transverse orientation using a B-mode ultrasound device (Technos MPX; ESAOTE S.p.A., Italy) and a 5-cm linear array probe (12.5 MHz; Fig. 1b). Ultrasound video was sampled at 25 Hz using an AD-video converter (Canopus ADVC-330, Grass valley) connected via a FireWire cable to a computer. During the scan, a single Optotrak 3020 system (Northern Digital, Waterloo, ON, Can-

ada) was used to track a 3-marker frame that was mounted to the probe. Position and orientation data were sampled at a frequency of 25 Hz. Prior to imaging, the setup had been calibrated by tracking a cross-point of two wires in a water cube. For that purpose, probe position and orientation were changed while keeping the cross-wire visible within the ultrasound video (Prager et al. 1998).

The protocol used for ultrasound scans was as follows. First, skin markers indicating the location of lateral and medial condyles were applied, as well as markers indicating the lateral and medial border of GM along its length (Fig. 1b, markers 1–4, respectively). Thereafter, a thick layer of gel (about 5 mm) was used to cover the scanning area, thereby increasing the probe contact surface area and minimising pressure exerted on the skin and underlying muscles. At the start of the scan, the probe was positioned at a longitudinal orientation with respect to the GM, slightly lateral to the lateral condyle. Next, without changing orientation, the probe was moved towards the medial condyle. Subsequently, probe orientation was changed to being transverse with respect to GM, and the scan continued within the borders drawn on the skin towards the most distal part of the Achilles tendon (Fig. 1b, marker 6).

Post-experimentally, using software custom-programmed in MATLAB, ultrasound probe position, orientation and video output data were used to create a 3D image of the scanned muscle (Gee et al. 2004). Based on the probe position and orientation, 2D ultrasound images consisting of pixels with grey values were placed within a designated 3D volume consisting of voxels (3D pixels). Voxels that were left empty were completed by nearest-neighbour interpolation of nearby assigned voxels (Gee et al. 2004).

Electromyography (EMG)

During gonio-dynamometer and ultrasound measurements, surface EMG of the tibialis anterior (TA) and GL muscles was collected in order to quantify muscle excitation. For the ultrasound measurement, we needed the surface of the GM to be free of electrodes, and we assumed activity levels in both heads of the gastrocnemius to be similar. The preparation of the skin and placements of the EMG electrodes was performed according to SENIAM instructions (Freriks et al. 1999). According to SENIAM instructions, electrode longitudinal position was set at 1/3 the distance from origin to insertion. Based on palpation, the electrodes were positioned at the centre of the muscle width. Using a multichannel system (MOBI; TMS-International, The Netherlands), EMG signals were A/D converted at 1024 Hz and synchronously recorded on a PC.

Prior to gonio-dynamometer and ultrasound measurements, participants were asked to perform a 5 seconds isometric maximal voluntary contraction (MVC; against resistance supplied by the assessor) towards dorsal and plantar flexion. During this MVC, participants lay prone on the table while the footplate angle was kept perpendicular to the tibia (i.e. at 0 ° angle). Post-experimentally, EMG signals recorded during gonio-dynamometer and ultrasound measurements were high-pass filtered at 20 Hz, to suppress movement artefacts, rectified and subsequently low-pass filtered at 5 Hz, to obtain the envelope. Filtered signals for TA and GL activity during gonio-dynamometer and ultrasound measurements were normalised for peak TA and GL MVC, respectively [EMG (%MVC)]. To minimise the effects of muscle excitation, data from gonio-dynamometer and ultrasound measurements were excluded from analysis if normalised peak EMG values exceeded 10% of MVC.

Data analysis

Externally applied footplate moments and resulting footplate rotation

Data obtained during gonio-dynamometer measurements were averaged over five trials for each condition for each participant individually.

Variables of GM geometry

Using a custom-made image analysis tool, programmed in MATLAB (version 7.1; The Mathworks), variables of muscle geometry were measured (described in detail in Bénard et al. 2011). The mid-longitudinal plane of the muscle belly was determined by placing markers at the following tree locations (Fig. 1c, markers 7–10, respectively). Within the transverse plane, a first marker was positioned at a ¼ distance between the most prominent aspects of the medial and lateral femur condyles. The position of this marker serves as a representative of the most proximal part of the muscle belly, thereby neglecting the fact that the origin of the GM runs

Fig. 1 Diagram of set-up of gonio-dynamometer and ultrasound measurements. (a) Exerting moments: lower right-leg is shown in a lateral sagittal view. This leg is supported in a horizontal orientation. The foot is fixed to the foot-fixation, which in turn is rigidly connected to the hand-held gonio-dynamometer. The dynamometer is used both to apply an external moment and consequently measure the corresponding degree of sagittal footplate rotation. During the exertion of moments and measuring resulting footplate angle, the angle-fixator is not used. (b–d) Details of 3D ultrasound recordings. For scans with the ultrasound probe, the footplate angle is fixed with the angle-fixator at angles corresponding to those recorded during exertion of 0 and 6 Nm dorsal flexion. (a) An example of a path of the scan of ultrasound probe. The scan starts at the lateral femur condyle (marker 1), and continues towards the medial condyle (marker 2). Then, the probe is rotated to image gastrocnemius medialis (GM) transversally, and the scanning path continues through the middle between lateral and medial markers (3 and 4) indicating GM borders towards the most distal part of the muscle belly (marker 5), subsequently continuing along the Achilles tendon to the calcaneus marker (6). (b) Three orientation markers are used to determine the mid-longitudinal plane: at ¼ distance between the medial (marker 2) and lateral (marker 1) most prominent point of the femur condyles was used to determine the GM origin (7), at the most distal part of the muscle belly (8), and at a line perpendicular to the tangent of the distal aponeurosis in the transverse plane (dotted line near marker 8) (9). An additional marker is placed at the central intersection of the Achilles tendon and the calcaneus to measure tendon length (10). (c) Measurement of muscle geometry within the GM. In steps: (1) muscle belly length (ℓm), i.e. between the origin and muscle–tendon junction; (2) tendon length (ℓt) from the distal end of the muscle belly to the calcaneus bone; (3) ℓfasc is calculated at 1/3 of the muscle belly, with the chosen orientation and the inclination between the specified proximal and distal aponeurosis; (4) fascicle–aponeurosis angle γ(fasc), being the mean of the angle between the fascicle line and the proximal and distal aponeurosis; (5) aponeurosis length (ℓa), determined as the longest side of the parallelogram (planimetric muscle model) constructed [consisting ℓm, ℓ(fasc) and γ(fasc)]; (6) length component of physiological cross-sectional area (ℓAf), perpendicular to both fascicle line and extrapolated aponeurosis line. (d) Planimetric muscle model in which all geometric variables are displayed on site.

into the popliteal fossa. The second marker was positioned at the most distal end of the GM muscle belly in the middle of the distal aponeurosis within the transverse plane. The third marker was placed within the same transverse plane perpendicular to the distal aponeurosis from the second marker. Based on a cadaver study by Bénard et al. (2009), the plane composed of these three markers has proved to be a good estimate of the orientation of the mid-longitudinal plane regardless of individual variation of GM detailed anatomy. Finally, within the transverse plane a final marker was placed at the attachment point of the Achilles tendon (most proximal) onto the calcaneus bone allowing measurement of tendon length. Repeatability of finding the target plane within the 3D reconstruction was tested in a pilot study. Two consecutive scans were compared for five subjects. Repeatability was expressed in terms of the coefficient of variance of distance between the anatomical landmarks [COV = (SD/mean)*100%]. The results revealed a high repeatability COV = 1.00% (range: 0.36–1.54%).

Within the GM mid-longitudinal plane, muscle geometry variables were assessed (Fig. 1d). (i) Within this plane at a distance corresponding to $^{2}/_{3}$ of muscle belly length from the estimated origin, between the proximal and distal aponeurosis, a line was plotted and rotated as a visual aid to match orientation of the target muscle fascicles. (ii) For measurements of fascicle length, five markers were positioned on both the proximal and distal aponeurosis surrounding the intersection with the target muscle fascicle. To determine aponeurosis orientations, polynomials were plotted best fitting the five markers for each aponeurosis. Using the marked locations, the following variables were assessed and calculated within the mid-longitudinal plane constituting a modelled parallelogram (planimetric muscle model; Van der Linden et al. 1998a;

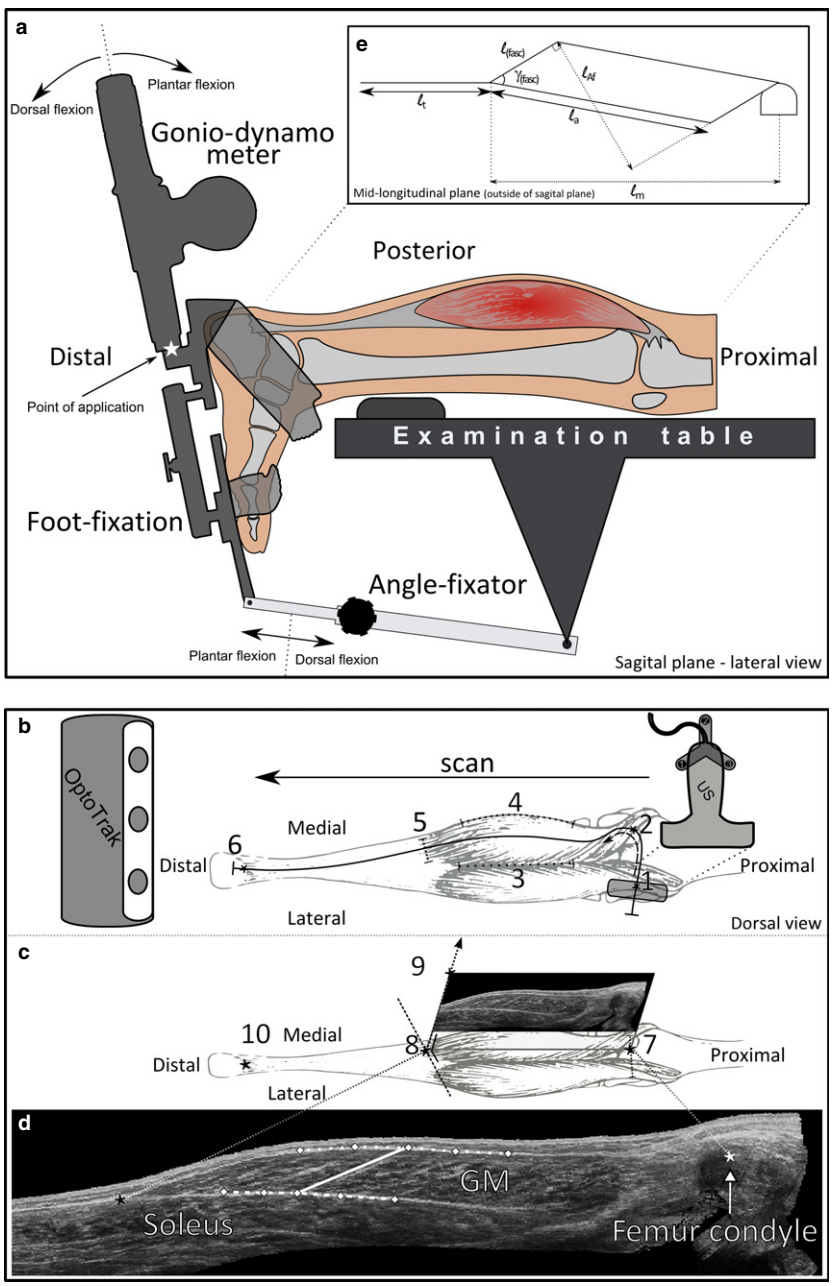

Fig. 1e): (i) muscle belly length (ℓm), i.e. distance between estimated origin and distal end of the most distal fascicle; (ii) ℓ(fasc) calculated as the distances along the line representing the fascicle and its intersection with the fitted polynomials; (iii) fascicle aponeurosis angle γ(fasc) being the mean of: (a) the sharp angle between the fascicle line and the tangent of the polynomial at the intersection with the distal polynomial; and (b) the sharp angle between the fascicle line and the tangent of the polynomial at the intersection with the proximal aponeurosis polynomial; (iv) aponeurosis length (ℓa), determined as the longest side of the modelled parallelogram constructed by ℓm, ℓ(fasc) and γ(fasc); (v) the length component of the physiological cross-sectional area (ℓAf), being the sum of all fibre diameters within the muscle including associated extracellular matrix materials within the mid-longitudinal plane (Fig. 1e; Van der Linden et al. 1998b); and (vi) muscle–tendon complex length, being the distance between the representation of the most proximal part of the muscle belly and the most proximal attachment point of the Achilles tendon on the calcaneus.

A pilot study for the present subject population indicated that making use of more than three independent estimates of the mid-longitudinal plane, standard variation did not decrease further. Within each selected plane, three analyses of muscle geometry were used in further statistical analysis, so in total nine variables were calculated. Standard deviations of variables of muscle geometry (within each individual) were relatively small (max < 9%, on average) and did not decrease any further when a higher number of estimates was made. An additional pilot study showed high repeatability (expressed in terms of coefficient of variation) in variables of muscle geometry measured post-experimentally between two reconstructed scans (COV about 4% in both fascicle length and pennation angle).

Statistics

Relationships between anthropometric variables and age were examined by linear regression analyses, and assessed using scatter plots. Regression line slopes and Pearson's coefficients of correlation were calculated using SPSS (version 20.0; SPSS). The relationships between dependent variables of muscle geometry [i.e. ℓm, ℓt ℓ(fasc), γ(fasc), ℓa, ℓAf] and independent variable age were examined using generalised estimating equations techniques (GEE; SPSS, version 20.0; SPSS), allowing correction for dependency of repeated measures of one factor (i.e. condition), and were used to test for main effects of net ankle moments and age. In addition to age, tibia length plays an important role in muscular development of adolescents. In order to examine the effects of tibia length on muscle development, length variables of muscle geometry were normalised for tibia length. GEE was also used to test for significant effects of age on normalised dependent length variables ℓm/ℓtib, ℓt/ℓtib, ℓ(fasc)/ℓtib, ℓa/ℓtib, ℓAf/ℓtib and independent variable age. The level of significance for all statistics was set at $P < 0.05$.

Table 1 Comparison of 2D and 3D ultrasound imaging results to anatomical measurements.

Cadaver	Method	ℓ(fasc) (cm)	γ(fasc) (°)
1	Section	4.17	12.09
	2D ultrasound	3.95 (−5.3%)	10.12 (−16.3%)
	3D ultrasound	4.19 (+0.4%)	10.65 (−11.9%)
2	Section	3.40	28.33
	2D ultrasound	4.24 (+24.8%)	25.60 (−9.6%)
	3D ultrasound	3.48 (+2.48%)	29.79 (+7.9%)

Results

Anthropometric variables

Sixteen male adolescent Caucasian subjects (mean age ± SD: 15.2 ± 3.1 years, ranging from 10 to 19 years) participated in this study.

Body mass, body height and tibia length increased by 4.2 kg year^{-1}, 4.2 cm year^{-1} and 0.8 cm year^{-1}, respectively (Table 2: Fig. 2). With age, for every 1 cm increase in body height, body mass increased by 1.0 kg. For each 1 cm gain in tibia length, body mass increased by 5.2 kg.

Degree of muscle excitation

During gonio-dynamometer and ultrasound measurements, EMG activity recordings were used to quantify muscle excitation. For all participants, maximal muscle excitation of both TA and GL ranged between 0.3 and 7.9%MVC, and mean ± SD = 1.2 ± 1.1%MVC. Such low levels of muscle excitation scored well below the criterion *a priori* set at 10%MVC.

Potential contributions of foot deformation to changes in footplate angle

To check for potential age-related changes in contributions to dorsal flexion footplate rotation by deformations of fore- and midfoot, the following arguments were considered. If growth of tibia lengths was the only factor considered, muscle–tendon complex length (ℓm+t, being the sum of muscle belly and tendon length) normalised for tibia length (ℓm+t/ℓtib) should attain equal values for equal footplate angles at different ages, unless some changes in footplate angle were allowed by acute foot deformation (Huijing et al. 2013). At a footplate angle = 0 °, ℓm+t/ℓtib did not differ ($P = 0.59$) between the younger (10–14 years) and older subjects (15–19 years) in the adolescent group (Fig. 3). Therefore, we have no indication that potential contributions of deformation of fore- and midfoot at dorsal flexion footplate angles change as a function of age.

During adolescence, dorsal flexion range of motion decreased significantly (Fig. 4). Footplate angles corresponding to externally applied 4 and 6 Nm (dorsal flexion) decreased significantly by −1.03 and −0.99 ° per year, respectively (Fig. 4). In contrast, footplate angles at 0 and −4 Nm (plantar flexion) were not age-related (Table 3; Fig. 4).

Adolescent growth; effects on variables of GM geometry

Adolescent growth is accompanied by increases of GM belly length at a rate of 0.5 cm year^{-1} (Fig. 5a). During adoles-

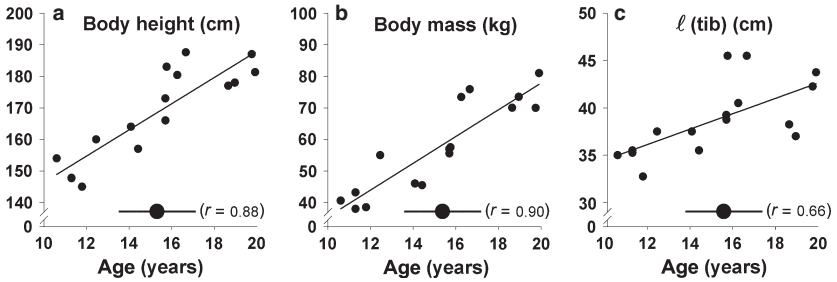

Fig. 2 Growth-related changes of anthropometrical variables of adolescent boys as a function of age. (a) Body height (cm), (b) body mass (kg) and (c) tibia length (cm) [ℓ(tib)]. All of the presented anthropometric variables changed significantly with factor adolescent age. The correlation coefficient *r* with adolescent age is shown for each anthropometric variable.

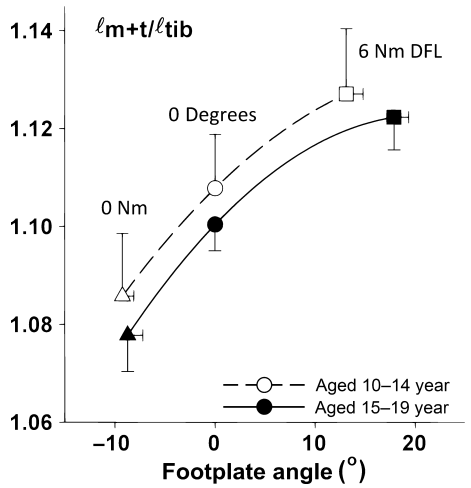

Fig. 3 Test for the effects of age on potential effects of foot deformation on footplate angles. It has been shown by Huijing et al. (2013) that deformation within mid- and forefoot potentially contributes to changes in dorsal flexion footplate angle. This would cause differences in muscle–tendon complex lengths when compared at equal angles. However, differences in tibia length between the youngest and oldest participants (see also Fig. 2c) would create similar inequalities that should, however, be removed after normalisation for tibia length. Mean values and SE of muscle–tendon complex length normalised for tibia length (ℓm+t/ℓtib) are plotted as a function of footplate angle. Footplate angle is presented as the deviation from its value with the tibia bone perpendicular to the footplate. At footplate angle = 0 °, ℓm+t/ℓtib did not differ ($P = 0.59$) between the younger (10–14 years) and older subjects (15–19 years) of the adolescent group. Therefore, we have no indication that potential contributions of deformation of fore- and midfoot at dorsal flexion footplate angles change as a function of age.

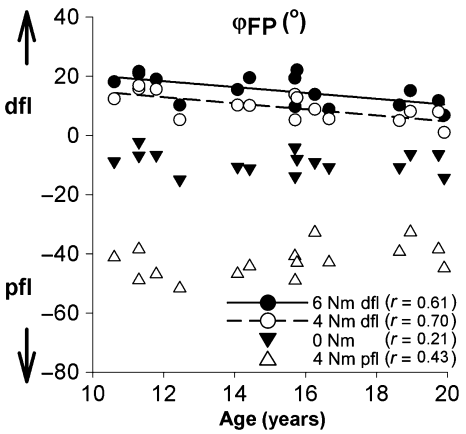

Fig. 4 Externally applied ankle moments and induced footplate rotation. Induced footplate angles at 6 Nm dorsal, 4 Nm dorsal, 0 and 4 Nm plantar flexion are shown over age. Individual values are plotted, and the corresponding measured angles for 6 and 4 Nm dorsal flexion (dfl) changed significantly with age; whereas 0 and 4 Nm plantar flexion (pfl) did not change with age. Correlation coefficients *r* with age are shown for the four conditions.

cence, potential increases of ℓt are fully obscured statistically by substantial inter-individual variation not related to growth, so no significant effects could be shown. However, the data suggest that growth rates of 0.4 cm year^{-1} seem feasible (Fig. 5b), so that final judgement regarding tendon length should be deferred. The intramuscular length variables ℓAf and ℓa increased significantly with age (increases of 0.3 and 0.5 cm, respectively; Fig. 5d,e). However, ℓ(fasc) was not associated with age (Fig. 5c). As ℓ(fasc) is to be considered unchanged, major increases in ℓm can only be ascribed to net effects of geometric changes found in ℓAf and ℓa, and more minor possible effects of γ(fasc). The latter variable increased significantly (at a rate of 0.5 ° per year), which, if present in isolation, would yield small decreases of ℓm. The fact that γ(fasc) does increase indicates that effects of increasing ℓa are not sufficient to fully accommodate increases in summed fibre diameters (trophy) within the mid-longitudinal GM plane (Fig. 7).

Does segment length explain growth in muscular length variables?

Figure 6 presents length variables of GM normalised for tibia length. GEE indicates that a significant main effect cannot be shown for any of the length variables normalised for tibia length [ℓt/ℓtib, ℓa/ℓtib, ℓ(fasc)/ℓtib], with the notable exception of ℓAf, normalised for ℓtib. This indicates that effects of increasing Af (i.e. trophy) of muscle fibres as a function of age are explained by more factors than just tibia growth. Changes of other normalised length variables are quantitatively explained by tibia growth, unless true deviations from this principle are obscured by substantial variation of these variables inter-individually.

Table 2 For ages between 10 and 19 years, intercept at age 10 years and increases per year of anthropometrics and correlation coefficient *r* with age are presented.

Variable	Increase per year	Intercept at age 10 years	Correlation with age (*r*)
Age (years)	1	10	1*
Body height (cm)	4.2	146.4	0.9*
Body mass (kg)	4.2	35.5	0.9*
ℓ(tib) (cm)	0.8	34.5	0.7*

The increase and intercept values are based on regression analysis.
* = $p < 0.05$

Table 3 For ages between 10 and 19 years, intercept at age 10 years, and increases per year of standardised ankle moments and resulting footplate angles and correlation coefficient *r* with age are presented.

Condition	Increase per year	Intercept at age 10 years	Correlation with age (*r*)
$\varphi_{\text{dorsal 6 Nm}}$ (°)	−1.0	20.3	−0.6*
$\varphi_{\text{dorsal 4 Nm}}$ (°)	−1.0	15.0	−0.7*
$\varphi_{\text{0 Nm}}$ (°)	−0.2	−7.8	−0.2
$\varphi_{\text{plantar −4 Nm}}$ (°)	0.8	−46.6	0.4

* = $p < 0.05$

These results indicate that during adolescent growth, muscle belly length increases are mediated by fascicle trophy and concomitant increases of aponeurosis length and angle of pennation between muscle fibres and aponeurosis [γ(fasc)].

Discussion

In agreement with our hypothesis, our present results indicate that, during adolescence, GM muscle geometry adapts to changing functional demands by increasing the length component of the physiological cross-sectional area without changing fascicle length. Simultaneously, dorsal footplate angles measured at standardised conditions decrease. In contrast, footplate angles at standardised neutral and plantarflexion positions were not associated with age (Fig. 4).

Limitations of the study

The following limitations regarding the 3D ultrasound and gonio-dynamometer techniques are described extensively and discussed by Bénard et al. (2009, 2010, 2011).

1 Images obtained using 3D ultrasound have a lower spatial resolution than images obtained with 2D ultrasound.
2 Externally applied moments are measured on the footplate. Ideally, we would like to know the net moment at the talocrural joint.
3 The measured footplate angles at the standardised moments are not solely an effect of GM architecture.
4 Implicit assumption of homogeneity of fascicle-related variables (length and angle).

However, two additional limitations should be pointed out.

1 Comparing geometry during adolescence requires examination at a (at least similar) reference length. Ideally this length would be muscle optimum length (i.e. muscle length at which actively optimal force is attained). For adult plantar flexors, muscle optimum length was approximated (to be between $+15° < \varphi_{\text{footplate}} < +20°$; Sale et al. 1982). For adolescents, the joint ankle at which plantar flexor muscles attain optimum length is unknown and may even change with age. In order to properly determine *in vivo* muscle optimum length, new techniques need to be developed for determining *in vivo* sarcomere lengths. Until such time, we are limited to making comparisons with external conditions set as similar as possible, or not studying the phenomena at all.
2 Comparing anthropometric and geometric variables with chronological age during adolescence yields substantial variances (Nordentoft, 1964; Nottelmann et al. 1987), possibly caused by individual variation, and effects of factors such as pubertal stage or hormonal levels. These factors may confound results particularly with a cross-sectional study design, and to overcome effects of these factors, ideally a longitudinal study design should be executed. However, such an approach was not feasible for us at the present time.

Anthropometric changes during adolescence and implications for GM muscle adaptation

In our cross-sectional sample (10–19 years old), comparison of mean growth rates of body mass show that body mass increased four times with body height as a function of age. Such proportional growth rates resemble those reported for a large cohort of similar aged adolescents (WHO, 2007; body mass: 5 kg year^{-1} and body height: 3.87 cm year^{-1}). Comparison of anthropometric changes reported for children (5–12 years old) reveals that mean growth rates for body mass and height of children (3.9 kg year^{-1} and 5.78 cm year^{-1}, respectively; WHO, 2007) differ from adolescents. For each centimetre increase in body height, children gain 0.67 kg of body mass, while adolescents gain 1.29 kg body mass (according to WHO, 2007). This implies that with a comparable amount of body height growth, adolescents need to account for relatively twice as much body mass as children.

Comparison of tibia length growth of adolescents and children indicates substantial differences. Mean tibia growth rates for adolescents [0.97 cm year^{-1} (present data)] are half those of children (1.91 cm year^{-1}; Oeffinger et al. 2010; Bénard et al. 2011). Along with the decrease in body

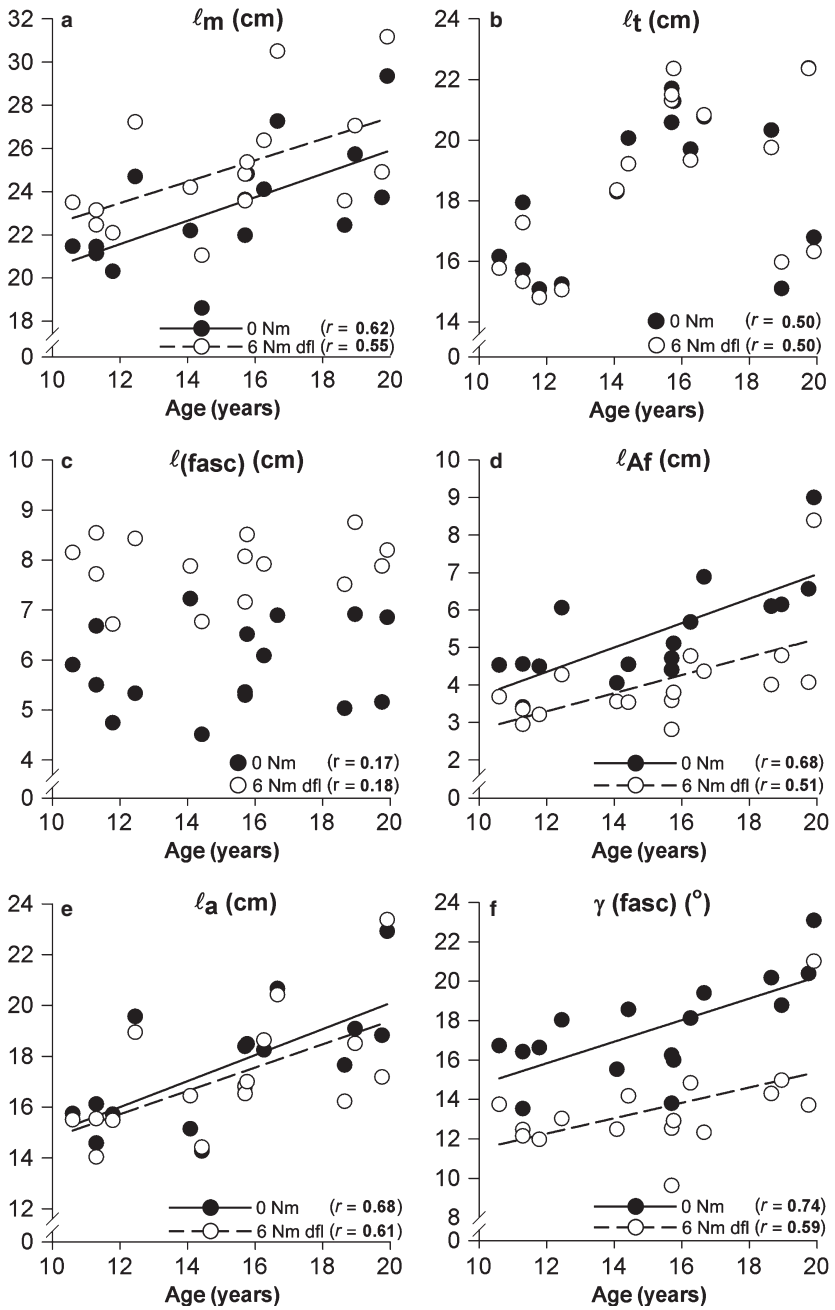

Fig. 5 Effects of age on GM geometry during adolescence at induced footplate angles corresponding to neutral (0 Nm) and 6 Nm dorsal flexion. A linear regression line is plotted, if a significant age effect is present, otherwise there was no regression line present. (a) Muscle belly length (ℓm), (b) tendon length (ℓt), (c) fascicle length [ℓ(fasc)], (d) fascicle angle with the aponeurosis [γ(fasc)], (e) aponeurosis length (ℓa), and (f) length component of physiological cross-sectional area (ℓAf). General estimated equations (GEE) indicated that all variables [except for ℓt and ℓ(fasc)] changed significantly with age. Correlation coefficients *r* with age are shown for geometry variables at both 0 and 6 Nm dorsal flexion.

height growth, tibia length growth decreases. With every 1 cm increase in tibia length, children gain 2.04 kg while adolescents gain 5.15 kg of body mass. To account for the higher body mass imposed moment's muscular adaptations are necessary to provide sufficient force over the muscle length range corresponding to daily life movements.

Geometrical adaptations in human GM during adolescence

Given the changes in body mass and tibia length during adolescence, it is expected that during adolescence GM muscle tendon–complex will increase its optimum length and physiological cross-sectional area (Morse et al. 2008; O'Brien et al. 2010). It has been postulated that muscle length is regulated such that muscle optimum length is attained at a joint angle at which the muscle is most frequently active (Herring et al. 1984; Huijing & Jaspers, 2005). Our present results regarding absolute GM muscle–tendon complex length at externally applied 0 and 6 Nm moments agree to a large extent with that postulation, as during adolescence GM length increased proportionally to tibia length. However, an increase in tendon length, as a function of age, could not be confirmed statistically. Even so, it is likely that such a lack of statistical evidence is caused by high individual variation of muscle belly and tendon

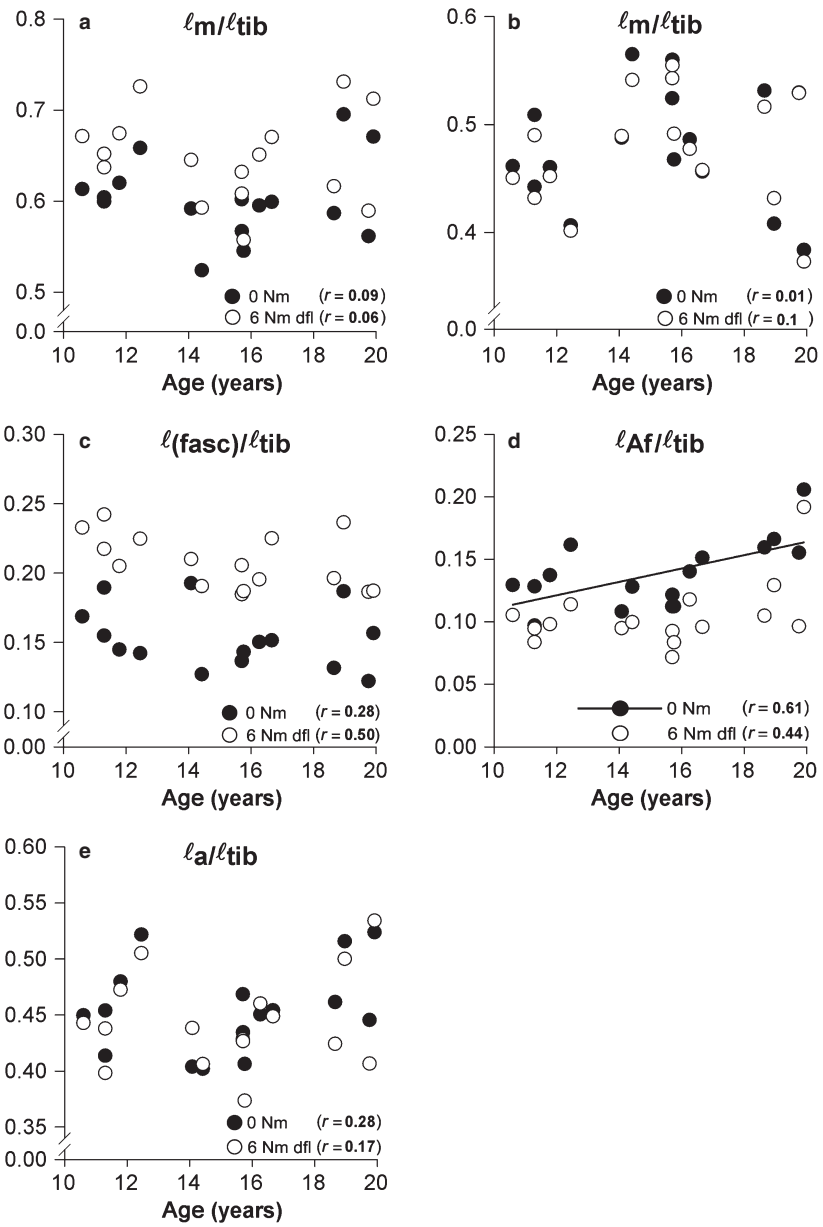

Fig. 6 Effect of age on GM geometry normalised for tibia length at induced footplate angles corresponding to neutral (0 Nm) and 6 Nm dorsal flexion. A linear regression line is plotted if a significant age effect is present, otherwise there was no regression line present. (a) Normalised muscle belly length (ℓm/ℓtib). (b) Normalised tendon length (ℓt/ℓtib). (c) Normalised fascicle length [ℓ(fasc)/ℓtib]. (d) Normalised length component of physiological cross-sectional area (ℓAf/ℓtib). (e) Normalised aponeurosis length (ℓa/ℓtib). Statistical analysis with GEE indicated that after normalisation only the normalised length component of the physiological cross-sectional area changed with age. Thus, tibia length cannot fully explain changes in ℓAf.

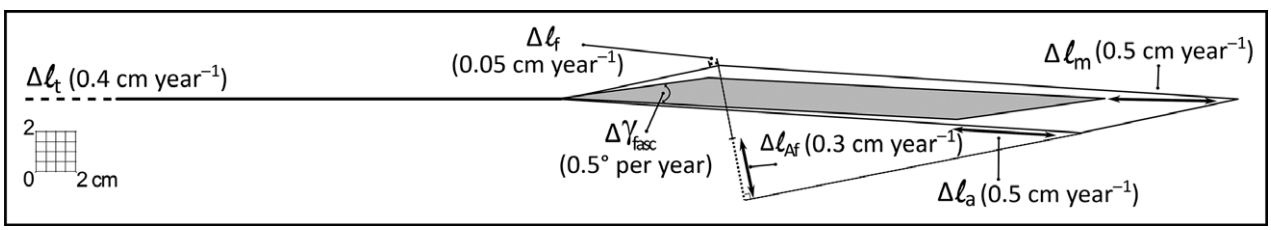

Fig. 7 Scaled planimetric model with growth rates in absolute values per year between 10 and 19 years: ℓm by 0.5 cm, ℓt by 0.4 cm (not significant), ℓ(fasc) by 0.05 cm (not significant), ℓAf by 0.3 cm, ℓa by 0.5 cm and γ(fasc) by 0.5 °.

lengths (e.g. comparatively short tendons observed in two subjects).

To determine how GM muscle belly adapts during adolescence, we measured variables of GM geometry at different ages. A major finding was that fascicle length did not change in subjects with increasing age. In contrast, for children, increases in ℓ(fasc) as well as ℓAf have been shown for GM (Bénard et al. 2011). It should be noted that, because of the very high degree of pennation of the GM, in addition to increases in fascicle length, ℓAf will also contribute to

muscle belly length (Swatland, 1980). However, finding high fascicle angles with the aponeurosis does not necessarily imply that the muscle is more pennate, as for the degree of pennation also angular orientation with respect to the line of pull (angle alpha) should be considered (Zuurbier & Huijing, 1993; angle alpha could also be small in combination with high values of fascicle angle with the aponeurosis; Willems & Huijing, 1992). Whenever the angle alpha is small, increases in ℓAf will not contribute much to increases in muscle belly length. The present results show that, during adolescence, ℓAf increases contribute substantially to GM length growth. Note that, ℓAf increases induced by trophy are more likely to occur than those induced by hyperplasia (cf. Rowe & Goldspink, 1969; Goldspink, 1972).

Most knowledge regarding changes in muscle geometry during adolescent growth is derived from studies conducted in young adult rats (Woittiez et al. 1986; De Koning et al. 1987; Heslinga & Huijing, 1990; Heslinga et al. 1995) of comparable human adolescent ages (cf. Quinn, 2005; rats reach sexual maturity at about 50 days and humans at about 11.5 years). Similar to our present findings, GM muscle belly length in adolescent rats was shown to increase due to trophy, as no increase in fascicle length was found (Woittiez et al. 1986; De Koning et al. 1987; Heslinga & Huijing, 1990). Muscle fibre lengths did not change as no sarcomeres in series were added. Apparently, addition of sarcomeres in series was not necessary as trophy-induced increases in muscle belly length matched increases in tibia length (Heslinga et al. 1995). In contrast to very pennate rat GM, less pennate rat m. soleus increased predominantly by the addition of sarcomeres in series as a result of the strain-induced ℓ(tibia) length growth (Heslinga et al. 1995). These studies imply that mechanical factors responsible for addition of serial sarcomeres with fibres of similarly strained muscle are less in very pennate muscle than a much less pennate muscle. Therefore, we conclude that the fascicle orientation affects the mechanism of muscular adaption.

Our present results are in accordance with results on muscle characteristics in human adolescents mainly focusing on muscle fibre size (trophy; Aherne et al. 1971; Vogler & Bove, 1985; Oertel, 1988). In boys aged 0–14 years, *post mortem* examination of gastrocnemius muscle shows that fibre size increased (by 124 μm^2 $year^{-1}$; Aherne et al. 1971). Different rates of increase were reported for different muscles (m. quadriceps, m. vastus lateralis, m. rectus femoris, m. deltoideus, m. biceps brachii; Aherne et al. 1971; Vogler & Bove, 1985; Oertel, 1988). However, rates of fibre size increase normalised for values at age = 10 years are quite similar, as shown by our calculations from these studies. Mean muscle fibre size growth after adolescence (> 19 years) stops (Lexell & Taylor, 1991; Lexell et al. 1992).

In vivo ultrasound data of boys and adults indicate that the muscle belly, tendon and fascicle length of the knee-extensors and GL adapt proportionally (Morse et al. 2008; O'Brien et al. 2010). Our finding is not in agreement with such results for the GM muscle. However, relative increases in physiological cross-sectional area precede increases in fascicle length in knee extensors as well as GL similar to our GM results, indicating that adult muscles are to be considered more suitable for force generation. Morse et al. (2008) conducted measurements on ultrasound images of GL in boys ($n = 11$, age = 10.9 ± 0.3 years) and men ($n = 12$, age = 25.3 ± 4.4 years). It should be noted that no information on moments exerted was considered. They reported that, *in vivo*, lengths of the muscle belly, tendon and fascicle adapt proportionally with muscle–tendon complex length allowing pennation angles [of fascicles with the aponeurosis γ(fasc)] to remain similar. For knee extensors, O'Brien et al. (2010) reported similar findings for such comparisons between men and boys. Our present findings are not in accordance with these reports. Despite the fact that a part of m. gastrocnemius has been the object of study in our work and that of Morse et al. (2008), such differences are quite likely affected by differences in muscle geometry, as well as in the functional role between these two different heads. The GL is less pennate and has longer fascicles (more serial sarcomeres) than GM, making the GL more suitable for activity at higher shortening velocities (Huijing, 1985; Maganaris et al. 1998; Abe & Fukashiro, 2001). In addition, the conditions of measurements may have contributed to the differences. For example, in order to reach 20 ° footplate dorsal flexion in our youngest subjects, we had to apply an external moment of 6 Nm. Because we found that the footplate angle corresponding to 6 Nm dorsal flexion decreased as a function of age, an even higher additional external moment (> 6 Nm) must have been applied by Morse et al. (2008) to attain the same footplate angle in adults. This makes it conceivable that, in their case, some acute stretching of fascicles may have confounded measurement of effects of longer term adaptation of fascicle length in adults. GM has to adapt to both length and force conditions altered by the effects of growth. However, during adolescence apparently increases in ℓAf match with GM length changes of the increased tibia length without persistent straining of muscle fibres that would lead to increases in serial sarcomeres numbers within fibres. In contrast, for children (5–12 years), having a less pennate GM (Bénard et al. 2011), increases of ℓAf are not sufficient to allow increases of ℓm and ℓt to match with longitudinal bone growth, inducing persistently higher muscle fibre strains, until this stimulus for addition of serial sarcomeres is removed by adding sarcomeres in series, which becomes apparent as higher fascicle lengths in ultrasound images.

Adaptation of GM geometry during adolescence affects footplate range of motion

During adolescence in males, dorsal flexion footplate angles (at 4 and 6 Nm) decrease by about 1 ° per year. With growth, decreasing ranges of motion are found commonly (Cheng et al. 1991; Vandervoort et al. 1992). Note, however, that

depending on the direction of movement, differences may exist, as we did not find any decrease in the footplate angle at plantar flexion (at −4 Nm applied external moment). Passive joint resistance may be affected by changes in joint capsules, ligaments and muscle–tendon complexes (Cheng et al. 1991; Latash & Zatsiorsky, 1993; Gajdosik et al. 1999). However, contributions of each of these structures to altering dorsal ranges of motion are still unknown. The contribution of GM to ankle joint stiffness has been quantified by several studies (Riener & Edrich, 1999; Silder et al. 2007). Within the muscle–tendon complex, joint resistance may be affected by intracellular elements; via cross-linking of actin–myosin filaments, titin filaments and collagen composition in connective tissues (i.e. tendons, aponeurosis, endomysia, perimysia and epimysia; Clark & Rogol, 1996; Gajdosik, 2001; Rogol et al. 2002; Hoang et al. 2007). A likely explanation for a decreasing footplate dorsal flexion range of motion, i.e. with GM increasing in ℓAf, is that resistance to muscle lengthening increases due to more parallel arranged materials.

In conclusion, in the cross-sectional sample, increases of tibia length and subsequent GM lengthening allow adaptation as a function of age to be mediated by increases of ℓAf. Simultaneously, dorsal footplate range of motion becomes smaller. Therefore, it is concluded that increases of ℓAf contribute both to longitudinal muscle belly growth, and to increased muscle and joint stiffness. The former is sufficient to match tibia length increases, so that long-term adaptation of fascicle length and presumably serial number of sarcomeres within muscle fibres is not necessary.

Acknowledgement

This study was financially supported by a grant from the Phelps Foundation for spastic disorders, Bussum, The Netherlands. The authors would like to thank Menno Bénard for his technical work during the pilot measurements.

Author contributions

G.W. conceived, designed and executed the experiments, analysed and interpreted the findings, and drafted and revised the article. P.A.H. and R.T.J. contributed to the design of the experiments, the analysis and interpretation of the findings, and draft and revision of the article. J.C.M. introduced G.W. to the experimental technique, and contributed to the design of the experiments and the revision of the article. J.G.B. judged the experiments and manuscript, particularly on clinical aspects, and contributed to the revision of the article. J.H. judged the experiments and manuscript particularly on technical aspects, and contributed to the revision of the article.

References

Abe T, Fukashiro S (2001) Relationship between sprint performance and muscle fascicle length in female sprinters. *J Physiol Anthropol Appl Human Sci* **20**, 141–147.

Aherne W, Ayyar DR, Clarke PA, et al. (1971) Muscle fibre size in normal infants, children and adolescents: an autopsy study. *J Neurol Sci* **14**, 171–182.

Bénard MR, Becher JG, Harlaar J, et al. (2009) Anatomical information is needed in ultrasound imaging of muscle to avoid potentially substantial errors in measurement of muscle geometry. *Muscle Nerve* **39**, 652–665.

Bénard MR, Jaspers RT, Huijing PA, et al. (2010) Reproducibility of hand-held ankle dynamometry to measure altered ankle moment-angle characteristics in children with spastic cerebral palsy. *Clin Biomech* **25**, 802–808.

Bénard MR, Harlaar J, Becher JG, et al. (2011) Effects of growth on geometry of gastrocnemius muscle in children: a three-dimensional ultrasound analysis. *J Anat* **219**, 388–402.

Cardoso HFV (2008) Epiphyseal union at the innominate and lower limb in a modern Portuguese skeletal sample, and age estimation in adolescent and young adult male and female skeletons. *Am J Phys Anthropol* **135**, 161–170.

Cheng JCY, Chan PS, Hui PW (1991) Joint laxity in children. *J Pediatr Orthop* **11**, 752–756.

Clark PA, Rogol AD (1996) Growth hormones and sex steroid interactions at puberty. *Endocrinol Metab Clin North Am* **25**, 665–681.

De Koning JJ, van der Molen HF, Woittiez RD, et al. (1987) Functional characteristics of rat gastrocnemius and tibialis anterior muscles during growth. *J Morphol* **194**, 75–84.

Freriks B, Hermens H, Disselhorst-Klug C, et al. (1999) The recommendations for sensor and sensor placement procedures for surface electromyography. In: Hermens H, editor. *European recommendations for surface electromyography*. Enschede: Roessingh Research and Development, 13–53.

Gajdosik RL (2001) Passive extensibility of skeletal muscle: review of the literature with clinical implications. *Clin Biomech* **16**, 87–101.

Gajdosik RL, Vander Linden DW, Williams AK (1999) Influence of age on length and passive elastic stiffness characteristics of the calf muscle-tendon unit of women. *Phys Ther* **79**, 827–838.

Gee A, Prager R, Treece G, et al. (2004) Processing and visualizing three-dimensional ultrasound data. *Br J Radiol* **77**, S186–S193.

Goldspink G (1972) Postembryonic growth and differentiation of striated muscle, *in* The structure and Function of Muscle, 2nd ed, Vol. 1. part 1. G.H. Bourne, editor, Academic Press, New York. 179–236.

Haines RW (1932) The laws of muscle and tendon growth. *J Anat* **66**, 578–585.

Herring SW, Grimm AF, Grimm BR (1984) Regulation of sarcomere number in skeletal muscle: a comparison of hypotheses. *Muscle Nerve* **7**, 161–173.

Heslinga JW, Huijing PA (1990) Effects of growth on architecture and functional characteristics of adult rat gastrocnemius muscle. *J Morphol* **206**, 119–132.

Heslinga JW, te Kronnie G, Huijing PA (1995) Growth and immobilization effects on sarcomeres: a comparison between gastrocnemius and soleus muscles of the adult rat. *Eur J Appl Physiol Occup Physiol* **70**, 49–57.

Hoang PD, Herbert RD, Todd G, et al. (2007) Passive mechanical properties of human gastrocnemius muscle tendon units, muscle fascicles and tendons *in vivo*. *J Exp Biol* **210**, 4159–4168.

Huijing PA (1985) Architecture of the human gastrocnemius muscle and some functional consequences. *Cells Tissues Organs* **123**, 101–107.

Huijing PA, Jaspers RT (2005) Adaptation of muscle size and myofascial force transmission: a review and some new experimental results. *Scand J Med Sci Sports* **15**, 349–380.

Huijing PA, Bénard MR, Harlaar J, et al. (2013) Movement within foot and ankle joint in children with spastic cerebral palsy: a 3-dimensional ultrasound analysis of medial gastrocnemius length with correction for effects of foot deformation. *BMC Musculoskelet Disord* **14**, 365.

Jaspers RT, van Beek-Harmsen BJ, Blankenstein MA, et al. (2008) Hypertrophy of mature Xenopus muscle fibres in culture induced by synergy of albumin and insulin. *Pflugers Arch* **457**, 161–170.

Kawakami Y, Abe T, Fukunaga T (1993) Muscle-fiber pennation angles are greater in hypertrophied than in normal muscles. *J Appl Physiol* **74**, 2740–2744.

Latash ML, Zatsiorsky VM (1993) Joint stiffness: myth or reality? *Hum Mov Sci* **12**, 653–692.

Lexell J, Taylor CC (1991) Variability in muscle fibre areas in whole human quadriceps muscle: effects of increasing age. *J Anat* **174**, 239–249.

Lexell J, Sjöström M, Nordlund ASA-S, et al. (1992) Growth and development of human muscle: a quantitative morphological study of whole vastus lateralis from childhood to adult age. *Muscle Nerve* **15**, 404–409.

Maganaris CN, Baltzopoulos V, Sargeant AJ (1998) *In vivo* measurements of the triceps surae complex architecture in man: implications for muscle function. *J Physiol* **512**, 603–614.

Morse CI, Tolfrey K, Thom JM, et al. (2008) Gastrocnemius muscle specific force in boys and men. *J Appl Physiol* **104**, 469–474.

Nordentoft EL (1964) Completion of growth in the lower limbs in relation to biological development menarche, and inherited factors. *Acta Orthop Scand* **34**, 213–224.

Nottelmann ED, Susman EJ, Dorn LD, et al. (1987) Developmental processes in early adolescence: relations among chronologic age, pubertal stage, height, weight, and serum levels of gonadotropins, sex steroids, and adrenal androgens. *J Adolesc Health Care* **8**, 246–260.

O'Brien TD, Reeves ND, Baltzopoulos V, et al. (2010) Muscle-tendon structure and dimensions in adults and children. *J Anat* **216**, 631–642.

Oeffinger D, Conaway M, Stevenson R, et al. (2010) Tibial length growth curves for ambulatory children and adolescents with cerebral palsy. *Dev Med Child Neurol* **52**, e195–e201.

Oertel G (1988) Morphometric analysis of normal skeletal muscles in infancy, childhood and adolescence: an autopsy study. *J Neurol Sci* **88**, 303–313.

Prager RW, Rohling RN, Gee AH, et al. (1998) Rapid calibration for 3-D freehand ultrasound. *Ultrasound Med Biol* **24**, 855–869.

Quinn R (2005) Comparing rat's to human's age: how old is my rat in people years? *Nutrition* **21**, 775–777.

Riener R, Edrich T (1999) Identification of passive elastic joint moments in the lower extremities. *J Biomech* **32**, 539–544.

Rogol AD, Roemmich JN, Clark PA (2002) Growth at puberty. *J Adolesc Health* **31**, 192–200.

Round JM (1999) Hormonal factors in the development of differences in strength between boys and girls during adolescence: a longitudinal study. *Ann Hum Biol* **26**, 49–62.

Rowe RW, Goldspink G (1969) Muscle fibre growth in five different muscles in both sexes of mice. *J Anat* **104**, 519–530.

Sale D, Quinlan J, Marsh E, et al. (1982) Influence of joint position on ankle plantarflexion in humans. *J Appl Physiol* **52**, 1636–1642.

Silder A, Whittington B, Heiderscheit B, et al. (2007) Identification of passive elastic joint moment-angle relationships in the lower extremity. *J Biomech* **40**, 2628–2635.

Swatland HJ (1980) Analysis of growth in a complex muscle (M. supracoracoideus, Anas platyrhynchos). *Growth* **44**, 139–146.

Van der Linden B, Koopman H, Grootenboer HJ, et al. (1998a) Modelling functional effects of muscle geometry. *J Electromyogr Kinesiol* **8**, 101–109.

Van der Linden B, Koopman H, Huijing PA, et al. (1998b) Revised planimetric model of unipennate skeletal muscle: a mechanical approach. *Clin Biomech* **13**, 256–260.

Vandervoort AA, Chesworth BM, Cunningham DA, et al. (1992) Age and sex effects on mobility of the human ankle. *J Gerontol* **47**, M17–M21.

Vogler C, Bove KE (1985) Morphology of skeletal muscle in children. An assessment of normal growth and differentiation. *Arch Pathol Lab Med* **109**, 238–242.

Watt KI, Jaspers RT, Atherton P, et al. (2010) SB431542 treatment promotes the hypertrophy of skeletal muscle fibers but decreases specific force. *Muscle Nerve* **41**, 624–629.

WHO Multicentre Growth Reference Study Group (2006) *WHO Child Growth Standards: Length/height-for-age, weight-for-age, weight-for-length, weight-for-height and body mass index-for-age: Methods and development*. Geneva: World Health Organization, 312 pages. Available at: http://www.who.int/childgrowth/standards/technical_report/en/, Accessed March 1 2014.

Willems ME, Huijing PA (1992) Effect of growth on architecture of rat semimembranosus lateralis muscle. *Anat Rec* **233**, 25–31.

Woittiez RD, Heerkens YF, Huijing PA, et al. (1986) Functional morphology of the M. gastrocnemius medialis of the rat during growth. *J Morphol* **187**, 247–258.

Zuurbier CJ, Huijing PA (1993) Changes in geometry of actively shortening unipennate rat gastrocnemius muscle. *J Morphol* **218**, 167–180.